The kinetics analyses of isothermal dehydration of PDMAA hydrogel by application of dispersive kinetics model

Branislav Stanković[1] 🄳

Abstract

The poly-*N*,*N*-dimethyl acrylamide (PDMAA) hydrogel was synthesized and its physicochemical properties were determined. The isothermal thermogravimetric curves of PDMAA hydrogel dehydration were measured at the five temperatures in the temperature range from 313 to 353 K. The apparent activation energy dependence on the dehydration degree was determined by Vyazovkin's isoconversional method. The conversion curves were fitted by the commonly-used equations for the processes with nucleation-limited steps. It was found that all conversion curves can be completely described by the acceleratory model equation of the dispersive kinetics model based on the Maxwell–Boltzmann distribution of activation energies. The dependencies of model equation parameters (*a* and *b*), the rate constant, and the activation energy on dehydration time were determined for all investigated temperatures. During the dehydration, the state of absorbed water within the hydrogel is changed continuously, relaxation processes within the hydrogel become faster and thus, dehydration nuclei with a bigger critical radius are formed, resulting in a decrease in the activation energy.

Keywords Hydrogel dehydration · Dispersive kinetics · Poly-*N*,*N*-dimethylacrylamide hydrogel · Time-dependent rate constant · Activation energy

Introduction

Hydrogels can be represented as a 3D network of hydrophilic polymers, which can reversibly absorb (swelling) and release (dehydration) a large fraction of aqueous solvent while maintaining the structure [1–3]. As such, hydrogels are an important class of so-called "smart" and "stimuli-sensitive" materials and have wide practical application in catalysis [4], tissue engineering [5], drug delivery [6], removal of water from fuels [7], biosensors [8], etc. There is relatively little research about the mechanism and kinetics of dehydration, albeit the swelling behavior and swelling kinetics of hydrogels have been lengthily studied [9–11]. Adnadjevic et al. modeled kinetics of the isothermal and non-isothermal dehydration of swollen poly(acrylic acid) hydrogel by the Weibull function of the dehydration times [12]. The Weibull function was also used by Stanković et al. to describe the kinetics of isothermal dehydration of alginate hydrogel [13]. The non-isothermal dehydration kinetics of poly(acrylic-co-methacrylic acid) hydrogel was mathematically described by the logistic function [14]. Liu et al. analyzed dehydration of chitosan fibers enhanced gellan gum hydrogel and concluded that its kinetics is composed of two stages, diffusion- and nucleation- limited [15, 16]. Ma et al. investigated polyvinylalcohol/polyvinylpyrrolidone/ hydroxyapatite/hydroxyapatite composite hydrogel. They found that dehydration kinetics consists of diffusion of water in the hydrogel network and evaporation [17]. Potkonjak et al. did a comparative analysis of isothermal kinetics of water evaporation and poly(acrylic acid)-g-gelatin (PAAG) hydrogel dehydration and showed that kinetics of both processes can be mathematically described by the novel dehydration nucleation model, by which dehydration does not occur through the release of individual water molecules, but instead by the formation (and release) of nuclei of the vapor phase from the potential nucleation centers [18]. This model was further used to describe the isothermal kinetics of PAAG hydrogel dehydration under microwave heating [19]. Stanković et al. investigated non-isothermal dehydration kinetics of PAAG hydrogel and found a procedure by which a distributed activation energy model can be connected with

✉ Branislav Stanković
branislav@ffh.bg.ac.rs

1 Faculty of Physical Chemistry, University of Belgrade, Studentski Trg 12-16, Belgrade, Serbia

the commonly-used kinetic model for solid-state reactions. It has been concluded that nucleation is the rate-limiting step for this process [20].

Skrdla and Robertson developed two semi-empirical equations of dispersive kinetics model (DKM) in which the distribution of activation energies is described by the Maxwell–Boltzmann function. One of these is the so-called deceleratory model equation, which can be used to describe processes with denucleation-limited step, whereas another is the acceleratory model equation, which has been derived in order to describe processes with nucleation-limited step [21]. Deceleratory model equation describes processes for which apparent activation energy increases during the course of the process (whereas the rate constant, consequently, decreases) and the opposite is true for the acceleratory model equation. The DKM of Skrdla and Robertson have been applied to various reactions and processes, such as phase transformation [21], reactions of pharmaceutical products [22] of, isothermal oxidation of synthetic soot [23], preparation [24], and self-assembly [25] of nanoparticles, solution-mediated reactions [26], absorption of gases [27], etc. Furthermore, throughout the detailed literature search, it has not been found that hydrogel dehydration kinetics is ever described by any of the above-mentioned equations, although, as it was previously said, nucleation is often the limiting step for dehydration kinetics of hydrogels.

Since properties of the hydrogel are closely related to the structure of water within it, water structure was widely investigated by various methods [28] and has been commonly described in the literature by the model of Jhon and Andrade [29] within which water exists in three states, i.e. as bound, intermediate, and free water. Bound water consists of the molecules that form relatively strong hydrogen bonds with polar groups of polymer chains, whereas free water is one that has a structure similar to the structure of bulk water, i.e. one for which interactions with molecules of a polymer are negligible. On the other side, intermediate water interacts weakly with polymer and its structure lies between the bound and free water. It is widely accepted that during dehydration free water evaporates first and that, only after that, comes to the evaporation of intermediate and bound water. Sekine and Ikeda-Fukazawa [30] investigated changes in the Raman spectrum of poly-*N,N*-dimethylacrylamide (PDMAA) hydrogel during dehydration. They found that, during the dehydration, vibration frequencies of water molecules and the ratio between water molecules with four hydrogen bonds and water molecules with two hydrogen bonds increase, (at first slowly, then sharper, and at the end of the process even sharper). This finding is in accordance with the model of Jhon and Andrade and suggests that changes in the Raman spectrum of hydrogel (i.e. water within it) become significant at the moment in which intermediate and bound water start to leave the hydrogel, which is related to

the weakening of the hydrogen bonds between water and polar groups in the polymer. Using the XRD method, Naohara et al. confirmed that during the dehydration of PDMAA hydrogel, the structure of water changes in the same way that Sekine and Ikeda-Fukazawa stated [31]. Having in mind that changes in water structure during the isothermal dehydration of PDMAA hydrogel are well investigated, the aim of this paper is to find a model which can describe the kinetics of this PDMAA hydrogel dehydration and thus, get a deeper insight into the dehydration mechanism. Furthermore, the understanding of dehydration mechanism and consequently water structure within PDMAA hydrogel is important since PDMAA is a widely used hydrophilic biocompatible polymer that found applications in molecular biology (such as DNA sequencing), as well as in medicine and pharmacology, where most remarkable uses are those in contact lenses and in drug delivery [32]. In the following sections, we will discuss the synthesis and some basic characterization of PDMAA hydrogel, after which kinetic analysis of isothermal dehydration will be done based on thermogravimetric measurements. Apparent activation, as one of the kinetic parameters, will be estimated by Vyazovkin's isoconversional method. The deeper kinetics analysis will be done from the point of view of a kinetics model which can well describe conversion curves. Finally, based on these results, the dehydration mechanism and water structure will be discussed.

Materials and methods

Materials

N,N-dimethylacrylamide (DMAA, Sigma-Aldrich, Saint Louis, USA, 99%), *N,N′*-methylenebis(acrylamide) (MBAA, Sigma-Aldrich, 99%), potassium persulfate (KPS, Centrohem, Stara Pazova, Serbia, ≥ 99%), and *N,N,N′,N′*-tetramethylenediamine (TMEDA, Sigma-Aldrich, ≥ 99.5%) were used as the monomer, cross-linker, initiator, and catalyst, respectively. Distilled water, purged with nitrogen gas for 3 h before sample preparation, was used in all experiments.

Synthesis of PDMAA hydrogels

The procedure of synthesis goes as follows [30]. First, DMAA (2.97 g) and MBAA (0.138 g) were dissolved in water (30 mL) and after that TMEDA (24 µL) was added. Finally, a solution of KPS (0.03 g) in water (3.0 mL) was added to the reaction mixture (at 273 K and with continual stirring). The solution was poured into a Teflon mold, allowing free radical polymerization to occur for 20 h at the ambient temperature. The resulting gel-type products were taken out, cut into disks, and washed out with distilled water to

remove the remaining unreacted compounds. The water was changed every 2–3 h for 3 days, except overnight. Subsequently, the washed-out hydrogels were dried in an air oven at 60 °C until a constant mass was attained. The obtained products were stored in a vacuum desiccator until use. For this investigation, the obtained hydrogel was swelled to the equilibrium state in distilled water at room temperature.

Equilibrium swelling degree and structural characterization of the synthesized samples

The equilibrium swelling degree (SD$_{eq}$) of PDMAA hydrogel was measured by the gravimetric procedure [30]. Methods proposed by Gudeman and Peppas [33] were used to determine and calculate structural properties of synthesized samples (in dried form), i.e. density (ρ), average molar mass between the network crosslinks (M_c), crosslinking degree (ρ_c), and distance between the macromolecular chains (d). The structural properties of the synthesized hydrogel are presented in Table 1.

Fourier transform infrared spectroscopy (FTIR) measurements

The ATR-FTIR spectrum of dry PDMAA hydrogel, in the form, as is, was recorded on SHIMADZU IRAffinity-1 s, Japan; in the range of wavenumber from 700 to 4000 cm^{-1}, with 20 scan times, and at a resolution of 4 cm^{-1}.

Thermogravimetric measurements

The kinetics of hydrogel dehydration was analyzed by isothermal thermogravimetric (TG) analysis at five temperatures, 313 K, 323 K, 333 K, 343, K and 353 K. Mass losses of 20 ± 1 mg equilibrium swollen hydrogel samples were measured in platinum pans under nitrogen atmosphere and at a gas flow rate of 10 mL min^{-1} by TG Analyzer, TA Instruments, Model Q500, USA. The heating rate of 100 K min^{-1} was used to heat samples to the selected dehydration temperature and that temperature was maintained until the end of the process.

Calculation of the dehydration degree

The dehydration degree, α, was calculated as:

Table 1 Structural properties of the synthesized PDMAA samples

Property	SD$_{eq}$/g g^{-1}	ρ/kg m^{-3}	M_c/g mol^{-1}	ρ_c/mol dm^{-3}	d/nm
Value	10.5	1210	2.80×10^5	4.32×10^{-3}	595

$$\alpha = \frac{m_0 - m}{m_0 - m_f} \tag{1}$$

where m_0, m, and m_f refer to the initial, actual, and final mass of the sample, respectively.

Vyazovkin's isoconversional method

Values of apparent activation energy at certain values of α, $E_{a,\alpha}$, were estimated by the Vyazovkin's flexible integral isoconversional method [34], within which as the value of $E_{a,\alpha}$ is taken one for which the minimum of the following function is obtained:

$$\Phi(E_{a,\alpha}) = \sum_{i=1}^{n} \sum_{j \neq i}^{n} \frac{I(E_{a,\alpha}, t_\alpha(T_j))}{I(E_{a,\alpha}, t_\alpha(T_i))} \tag{2}$$

where the $t_\alpha(T)$ is the time by which the conversion degree α is reached at temperature T and $I(E_{a,\alpha}, t_\alpha(T))$ is:

$$I(E_{a,\alpha}, t_\alpha(T)) = \int_{t_{\alpha-\Delta\alpha}}^{t_\alpha} e^{-\frac{E_{a,\alpha}}{RT}} dt = e^{-\frac{E_{a,\alpha}}{RT}} \Delta t \tag{3}$$

Minimization of $\Phi(E_{a,\alpha})$ has been done by the Wolfram Mathematica program package.

Experimental data fitting

The conversion curves were fitted with deceleratory (Eq. 4) and acceleratory (Eq. 5) equations of DKM derived by Skrdla and Robertson [21]:

$$\alpha = 1 - e^{at\left(e^{-bt^2} - 1\right)} \tag{4}$$

$$\alpha = 1 - e^{-\frac{a}{t}\left(e^{bt^2} - 1\right)} \tag{5}$$

where α represents the conversion degree at time t, while a and b are (positive) fitting parameters of the model. Model parameters a and b have been obtained by the OriginPro program package and the Levenberg–Marquardt method that minimizes the reduced chi-square value and gives the adjusted R^2 value by which one can estimate the goodness of the fit.

Results and discussion

By its type, the synthesis of PDMAA hydrogel is free-radical crosslinking polymerization.

N,N'-methylenebis(acrylamide) is commonly used as a cross-linker for polymers based on polyacrylamide and its

derivatives. In order to better understand the structure of PDMAA hydrogel, let us first discuss the mechanism of its synthesis. Lazzari et al. [35], proposed the model for the acrylamide/N,N'-methylenebisacrylamide synthesis (Fig. 1a) which holds, due to its generality, in the case of PDMAA hydrogel synthesis. Before moving on to the mechanism itself, it is convenient to define notation for reacting species and the meaning of the indices in their subscripts. The model involves two types of monomers, mono- (in our case DMAA) and bi-functional monomer (in our case MBAA), which are denoted as M_1 and M_2, respectively. In the case of radicals, $R^{\cdot}$, the first index takes values of 1, 2, and 3 and defines its type, i.e. monofunctional, bifunctional, and one with pendant double bond, respectively. The second index corresponds to the chain length, whereas the third index is for the number of pendant double bonds. In the case of the

pendant double bond species, $D_{3,r,q}$, the meaning of indices is the same as for the radicals. Finally, for the resulting polymers, P, first and second index denote chain length and number of pendant double bonds, respectively. At the beginning of the polymerization process, it comes the initiation of both M_1 and M_2 monomers. Thus, two types of radicals are formed. The next step is the propagation of the polymer chain, which occurs in three ways: with M_1, with M_2, as well as with pendant double bond species. In the last case, it comes to the formation of one effective crosslinking. On the other side, reactions of primary and secondary cyclization consume one of the pendant double bonds, and thus crosslinking does not occur from that pendant double bond [35]. Primary cyclization forms a cycle within one primary polymer chain, whereas, in the case of secondary cyclization, a cycle is formed between two or more polymer chains
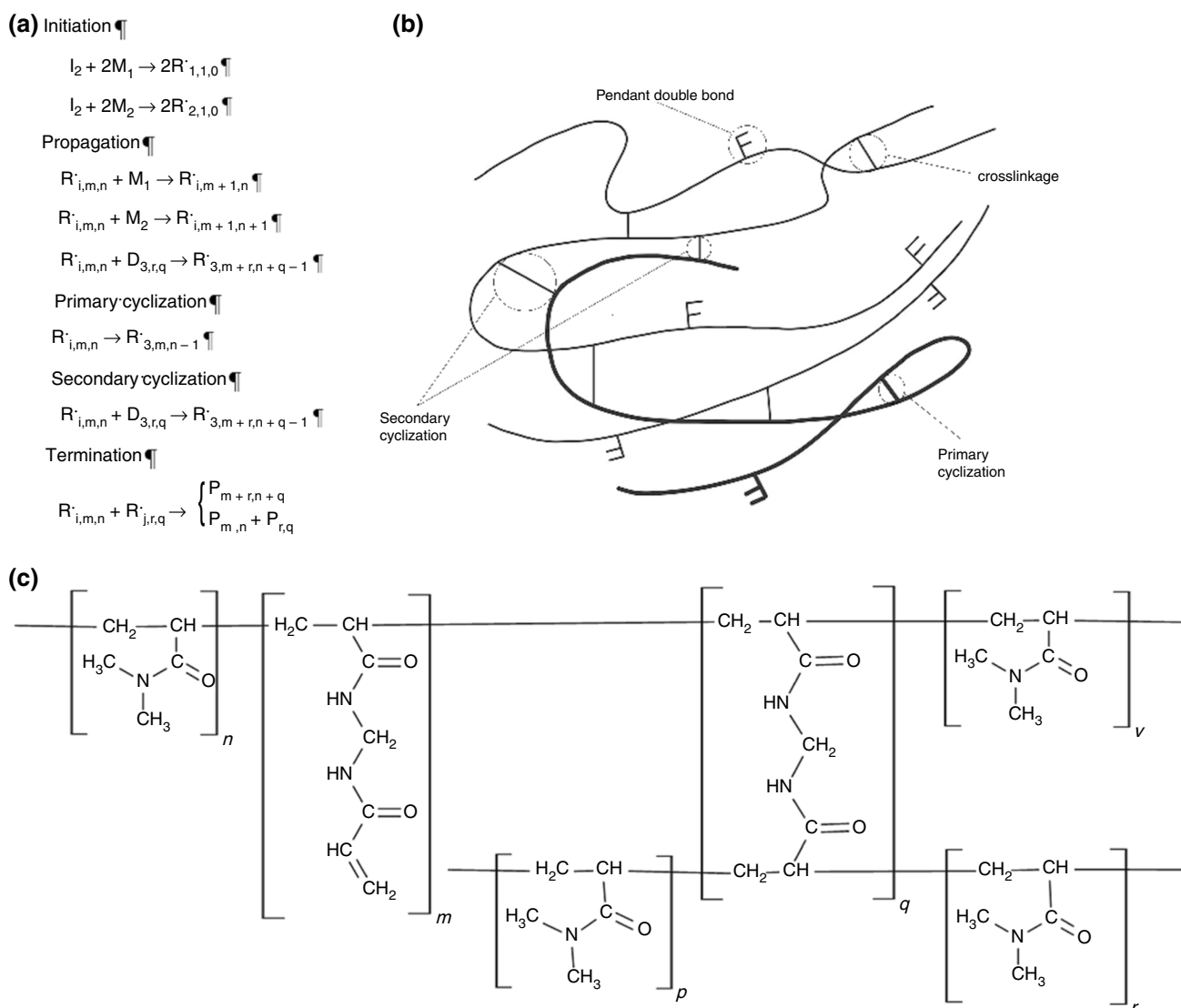
(a) Initiation

$$I_2 + 2M_1 \rightarrow 2R^{\cdot}_{1,1,0}$$

$$I_2 + 2M_2 \rightarrow 2R^{\cdot}_{2,1,0}$$

Propagation

$$R^{\cdot}_{i,m,n} + M_1 \rightarrow R^{\cdot}_{i,m+1,n}$$

$$R^{\cdot}_{i,m,n} + M_2 \rightarrow R^{\cdot}_{i,m+1,n+1}$$

$$R^{\cdot}_{i,m,n} + D_{3,r,q} \rightarrow R^{\cdot}_{3,m+r,n+q-1}$$

Primary cyclization

$$R^{\cdot}_{i,m,n} \rightarrow R^{\cdot}_{3,m,n-1}$$

Secondary cyclization

$$R^{\cdot}_{i,m,n} + D_{3,r,q} \rightarrow R^{\cdot}_{3,m+r,n+q-1}$$

Termination

$$R^{\cdot}_{i,m,n} + R^{\cdot}_{j,r,q} \rightarrow \begin{cases} P_{m+r,n+q} \\ P_{m,n} + P_{r,q} \end{cases}$$

(b)

(c)

Fig. 1 **a** Mechanism of synthesis, **b** schematic drawing and **c** chemical structure of PDMAA hydrogel

(Fig. 1b). The end of the chain propagation occurs in the termination step. Having mechanism in mind, the chemical structure of PDMAA hydrogel, as well as its schematic drawing, are presented in Fig. 1. The photos of dried, as well as the swollen PDMAA hydrogel, are given in Fig. 2. It can be seen that the dried sample has a granular structure, while the swollen sample is hydrogel with relatively high transparency.

In the FTIR spectrum hydrogel sample (Fig. 3) several characteristic peaks can be observed: ν_{as}, ν_s, and δ_s band of CH_3 group at 2892 cm^{-1}, 2832 cm^{-1}, and 1424 cm^{-1}, respectively; ν band of C=O group at 1632 cm^{-1}; δ band of CH_2 group from MBAA at 1504 cm^{-1}; ν band of CN group at 1256 cm^{-1}, and polymer skeletal vibrations at 1184 cm^{-1} (and lower wavenumber). The wavenumbers of the above-mentioned peaks are in the accordance with those of Raman spectra from [30], while the spectrum is similar to the ATR-FTIR spectra that can be found in the literature [36, 37]. Moreover, the lack of a peak around 800 cm^{-1} corresponding to the vibration of the C=C bond in DMAA and MBAA [36] further confirms that PDMAA hydrogel was synthesized.

Thermogravimetric curves showing the dehydration process of equilibrium swollen PDMAA hydrogel at different temperatures are presented in Fig. 4. For all temperatures of interest, the isothermal TG curves have a sigmoidal and asymmetric shape. Also, all curves are shifted to the right and, with an increase in temperature, they become less asymmetric and more sigmoidal.

As it is well known, the shape of the curve showing the rate of a process versus conversion degree can give us some basic information about the kinetics model of that process. Dependencies of the dehydration rate of PDMAA hydrogel on the dehydration degree at all temperatures are presented
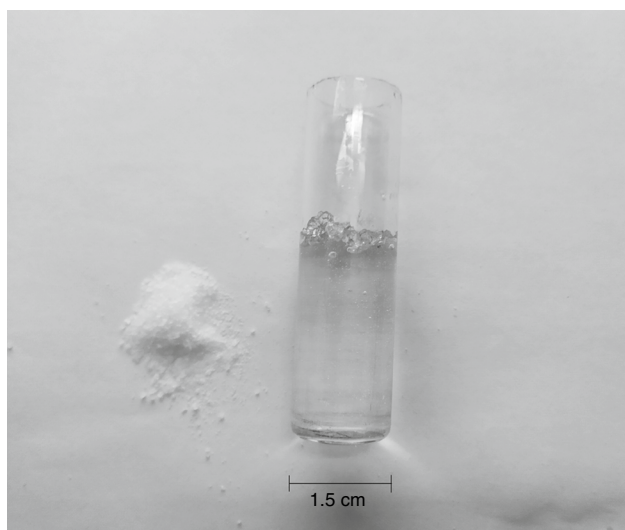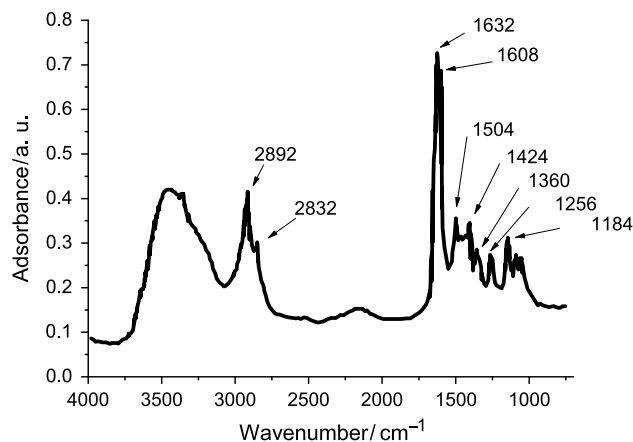

Fig. 3 FTIR spectra of PDMAA hydrogel

in Fig. 5. It can be seen that these curves have a shape of a wide peak. Also, with the increase in temperature, the maximum shifts toward higher values of α, and curves become more asymmetric. From the shape of the dependencies shown in Fig. 5, it can be seen that isothermal dehydration of PDMAA hydrogel has dependencies that are different from those which any of the commonly-used kinetic models in solid-state science has [38], although they mostly look like one corresponding to the nucleation model. Since reaction rate is the product of reaction model and rate constant, this further implies that dehydration kinetics cannot be described by any model within classic kinetics, and thus model which allows changes of rate constant during the process needs to be applied.

In order to estimate E_a dependence on α the Vyazovkin's isoconversional method was used. It can be seen that the

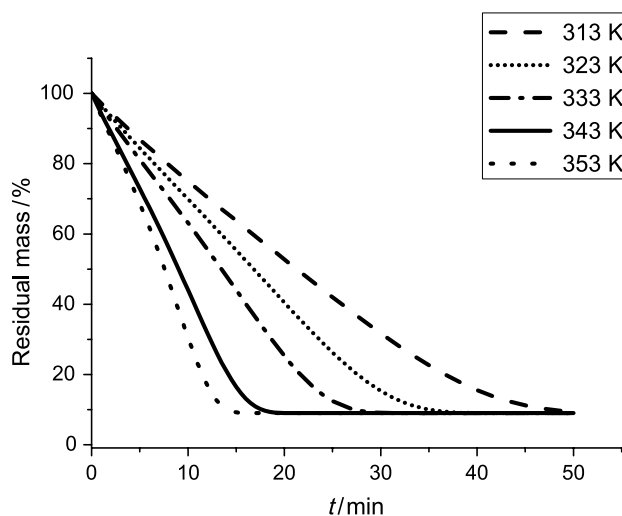**Fig. 2** PDMAA hydrogel in dry and swollen form

Fig. 4 The isothermal TG curves of PDMAA hydrogel dehydration at different temperatures
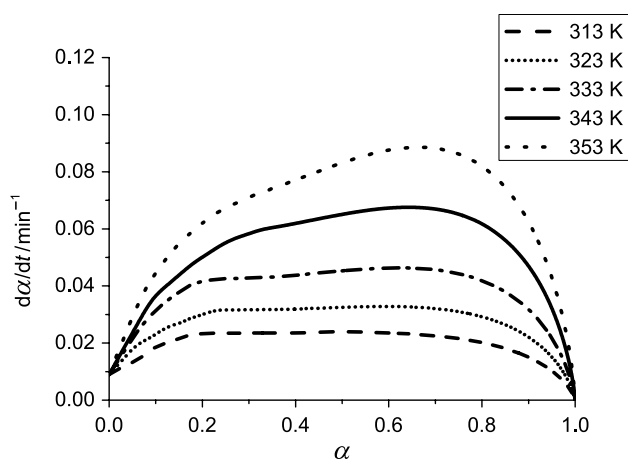
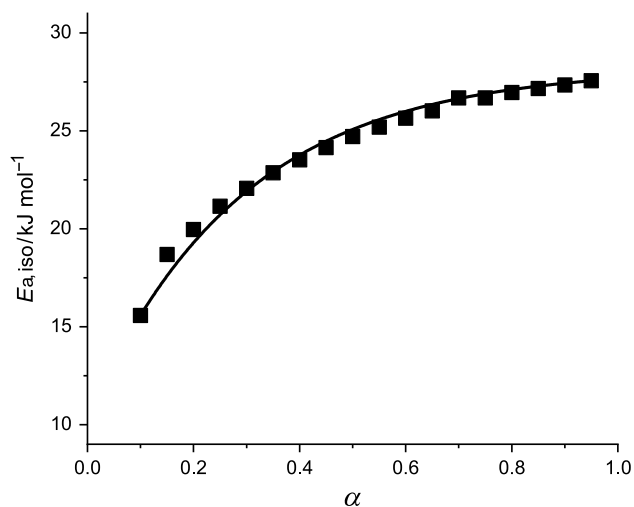**Fig. 5** The dependence of isothermal dehydration rate on dehydration degree

Fig. 6 Dependence of $E_{a,\,iso}$ versus α obtained by the Vyazovkin's isoconversional method (scatter) and fitting by equation $E_a(\alpha) = E_{a,max} - Ae^{-\frac{\alpha}{B}}$ (solid line)

value of activation energy obtained by isoconversional method, $E_{a,\,iso}$ increases concavely with α (Fig. 6). Moreover, it was found that $E_{a,\,iso}$ versus α curve can be fitted by the function $E_{a,\,iso}(\alpha) = E_{a,max} - Ae^{-\frac{\alpha}{B}}$, where $E_{a,max} \approx 28$ kJ mol^{-1} $A \approx 15.5$ kJ mol^{-1}, $B \approx 0.36$, and adj$R^2 \approx 0.992$. Parameters $E_{a,max}$, A, and B have no (strong) physical meaning, although form strictly mathematical point of view, $E_{a,max}$ is the value of activation energy when $\alpha \to \infty$, $E_{a,max}$-A is the value at the beginning of the dehydration (i.e. at $\alpha = 0$), and B is the inverse of the parameter related with the rate by which activation energy changes.

Since the value of $E_{a,\,iso}$ increases exponentially, the fitting of experimental data was initially done by the deceleratory equation (Eq. 4). It turned out that this equation cannot describe dehydration curves. This can be clearly seen from
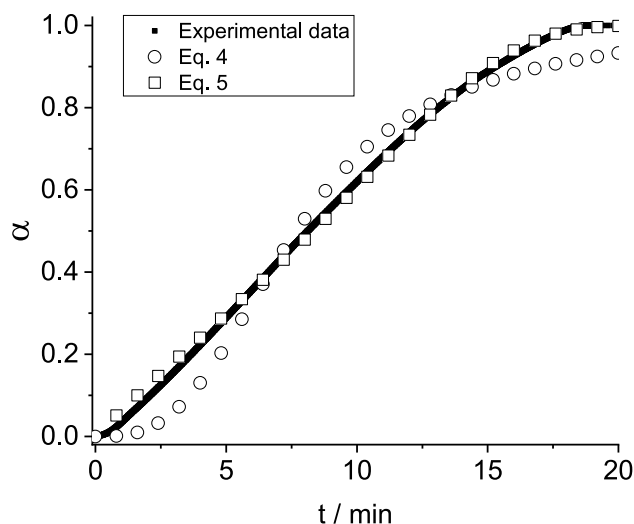

Fig. 7 The fitting of the dehydration conversion curve at 343 K with deceleratory (Eq. 4) and acceleratory (Eq. 5) equations of DKM

Fig. 7, where are presented experimental and deceleratory model curve for 343 K. In the papers of Liu et al. [15, 16], Potkonjak et al. [18], and Stanković et al. [20] authors found that nucleation is the rate-limiting step in the kinetics of hydrogel dehydration. Since, by the basic assumptions of DKM proposed by Skrdla and Robertson, nucleation-limited kinetics can be described by the acceleratory equation, PDMAA hydrogel isothermal dehydration kinetics was fitted by Eq. 5. As it can be seen (Fig. 7), this model equation is able to describe the kinetics of the dehydration process within the entire interval of time. Also, from a closer look at Table 2, where parameters of Eq. 6 and values of R^2 are presented, one can see that for all sets of experimental data, the value of R^2 is very high. Thus, one can conclude that PDMAA dehydration can be described by the acceleratory equation of DKM.

As can be seen from Table 2, with an increase in temperature, the value of a decreases, while the value of b increases. Since parameter a is defined as reciprocal of first-order rate constant and parameter b as the second-order rate constant [39], this finding clearly confirms that, at a higher temperature, the rate of dehydration is higher at every value of α (Fig. 5). On the other side, since values of parameter b are very low, it is expected that values of activation energy and rate constant should not significantly change with time. Moreover, it was found that parameters of model change exponentially, i.e. $a(T) = a_0 e^{-a_1 T}$ and $b(T) = b_0 + b_1 e^{-b_2 T}$. Values of a_0, a_1, b_0, b_1, and b_2, as well as values of $adjR^2$ for these exponential fits, are given in Table 3.

By knowing the values of parameters a and b, i.e. their dependence on temperature, one can calculate values of so-called global activation energy, E_a^0, and Arrhenius-like frequency factor, A, as well as obtain activation energy and

Table 2 Parameters of acceleratory model equation which fits PDMAA hydrogel isothermal dehydration kinetics at different temperatures

T/K	313	323	333	343	353
a/min	35.9 ± 0.2	21.1 ± 0.2	14.9 ± 0.2	8.6 ± 0.1	5.7 ± 0.1
b/min^{-2}	$(8.55 \pm 0.04)\,10^{-4}$	$(1.74 \pm 0.02)\,10^{-3}$	$(2.99 \pm 0.02)\,10^{-3}$	$(7.46 \pm 0.06)\,10^{-3}$	$(1.26 \pm 0.01)\,10^{-2}$
adjR^2	0.996	0.994	0.995	0.994	0.999

Table 3 Parameters obtained by fitting dependences of a and b on temperature by exponential functions

$a(T) = a_0 e^{-a_1 T}$			$b(T) = b_0 + b_1 e^{-b_2 T}$			
a_0/min	a_1/K^{-1}	adjR^2	b_0/min^{-2}	b_1/min^{-2}	b_2/K^{-1}	adjR^2
$(1.3 \pm 0.9) \times 10^8$	$(4.8 \pm 0.2) \times 10^{-2}$	0.997	$-(1.4 \pm 0.9) \times 10^{-3}$	$(7 \pm 2) \times 10^{-10}$	$(4.7 \pm 0.8) \times 10^{-2}$	0.997

rate constant dependencies on time. Values of E_a^0 and $\ln A$ were estimated from $\ln(a*b)$ versus $1/T$ curve. The value of $\ln A$ is the intercept of this linear dependence, whereas E_a^0 can be calculated as a product of the gas constant and the gradient. It was found that $E_a^0 \approx 20.8 \pm 0.2$ kJ mol^{-1} and $A \approx 89 \pm 1$ min^{-1}. Dependencies of activation energy obtained by DKM, $E_{a,\,DKM}$, on time (Fig. 8a) are calculated using Eq. 6 [39]:

$$E_{a,\,DKM} = E_a^0 - RTbt^2 \tag{6}$$

Since the mathematical form of dependence of α on t is known, it is possible to transform the dependence of $E_{a,\,DKM}$ on t into the $E_{a,\,DKM}$ versus α dependencies (Fig. 8b). From a closer look at Fig. 8a, it can be seen that in the beginning, the $E_{a,\,DKM}$ value is almost time-independent and close to the value of E_a^0. After that $E_{a,\,DKM}$ value decreases rapidly. At a certain value of time, $E_{a,\,DKM}$ value decreases with temperature, i.e. decrease in $E_{a,\,DKM}$ with time becomes more pronounced as the temperature increases. Further, from Fig. 8b, one can notice that when $\alpha < 0.2$, $E_{a,\,DKM}$ insignificantly changes with α, whereas when $\alpha > 0.2$, the decrease is more pronounced. At a certain α, $E_{a,\,DKM}$ decreases with temperature. Moreover, as it was previously said, Sekine and Ikeda-Fukazawa [30] investigated changes in the Raman spectrum of PDMAA hydrogel during dehydration. They found vibration frequencies of water molecules and a fraction of water molecules with four hydrogen bonds increase during dehydration. According to the here presented results of $E_{a,\,DKM}$ versus α dependencies, these changes become more pronounced at $\alpha \approx 0.2$.

It can be noticed that $E_{a,\,DKM}$ versus α curves have a completely different shape than the one obtained by the isoconversional method (Fig. 6). In the other words, although values of apparent activation energy are in relatively good agreement, values obtained by the isoconversional method increases, whereas those obtained by the dispersive kinetics model decrease. The underlying reason for this discordance
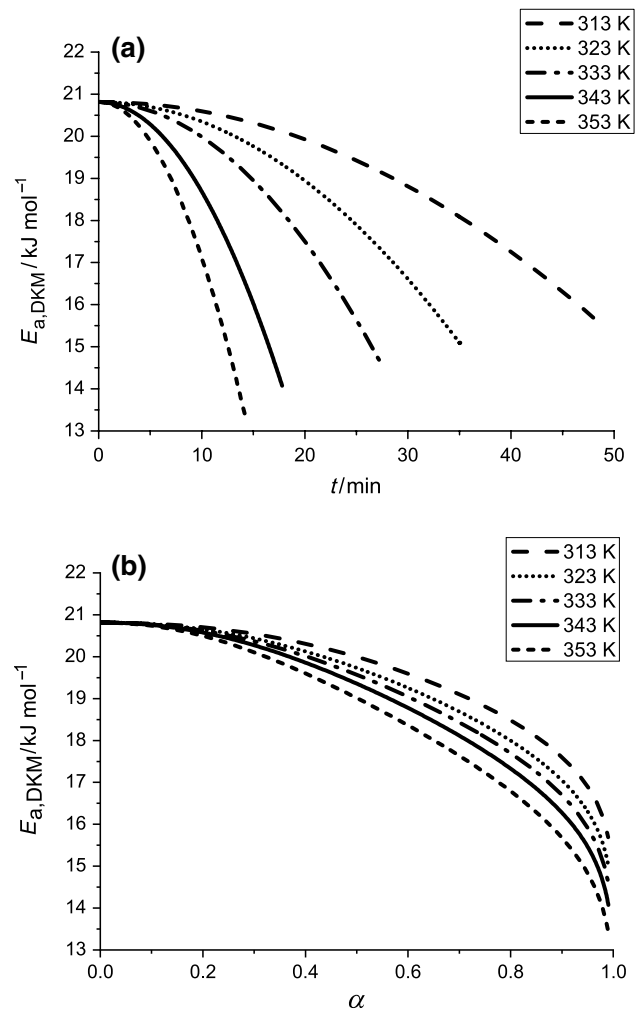

Fig. 8 Dependence of PDMAA dehydration activation energy on **a** time and **b** dehydration degree at different temperatures

is that (Vyazovkin's) integral isoconversional method assumes that the rate constant is only a function of T, but not of the α, which can lead to the misprediction of E_a values [40, 41].
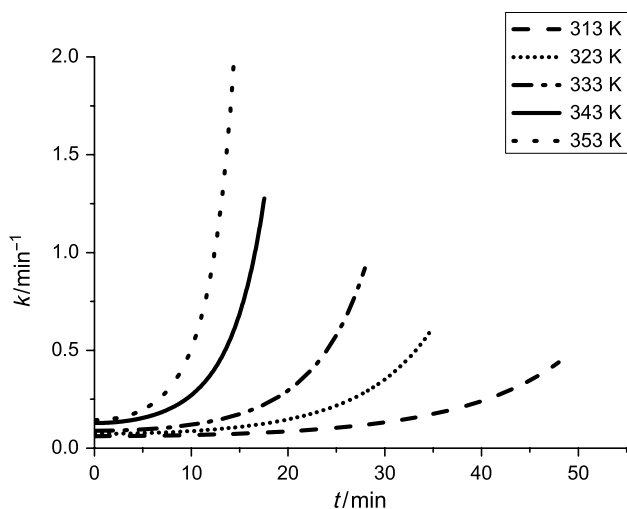
Fig. 9 Dependence of PDMAA dehydration rate constant on time at different temperatures

Taking into account Arrhenius equation and Eq. 6, the rate constant can be written as:

$$k = Ae^{-\frac{E_a^0 - RTbt^2}{RT}} = Ae^{-\frac{E_a^0}{RT}}e^{bt^2} \tag{7}$$

Furthermore, since the basic assumption of the DKM is that process has the first-order kinetics, Eq. 8 holds:

$$\alpha = 1 - e^{-\int_0^t kdt} \tag{8}$$

By involving k from Eq. 7 into Eq. 8, one can find that the following relation needs to be valid in order to α has a form given by Eq. 5 [39]:

$$a = \frac{A}{2b}e^{-\frac{E_a^0}{RT}} \tag{9}$$

Finally, by combining Eqs. 7 and 9, reaction constant as a function of time, containing only parameters of the model, can be obtained:

$$k = 2abe^{bt^2} \tag{10}$$

Note that Eq. 10 can be also obtained by differentiation of α (Eq. 5) on t and considering that process obeying the first-order kinetics. The dependence of the isothermal dehydration rate constant on time was calculated by Eq. 10 and presented in Fig. 9. As can be expected, the value of k is almost constant at the beginning of the process and then abruptly increases. Also, at a certain value of t, the k values increase with temperature. The change of k with time is more pronounced than those of E_a.

Since nucleation limited processes have been commonly described in the literature by various functions [18, 42],

such as logistic (Eq. 11), Weibull (Eq. 12), and Gompertz (Eq. 13), as the final step of examination of the PDMAA dehydration kinetics, the dehydration conversion curves were fitted by these three functions. In Fig. 10 presented are experimental and model curves for 343 K. As can be seen, all functions describe α versus t curve well. Moreover, by comparative analysis of Figs. 7 and 10, one can see that DKM and Gompertz function are equally good (in accordance with which are the nearly same values of adjR^2, i.e. 0.994).

$$\alpha = 1 - \frac{1}{1 + e^{a+bt}} \tag{11}$$

$$\alpha = 1 - e^{-\left(\frac{t}{\eta}\right)^\beta} \tag{12}$$

$$\alpha = 1 - e^{ae^{bt}} \tag{13}$$

Weibull, Gompertz, logistic and acceleratory DKM functions can be written in the form so that they describe process obeying first-order kinetics, where the reaction rate is changed due to the formation of nuclei with different critical radius during the dehydration [24, 39], although mathematical forms of k versus t are significantly different (Eqs. 14–16). Thus, in order to properly address the above-observed finding (i.e. similarity in the goodness of the fit) and to clarify DKM is the most suitable for the modeling of kinetics itself, k versus t dependencies (Fig. 11) were calculated and compared with one obtained from the experimental curve. It is clear that only the DKM model gives proper values of rate constant (and thus apparent activation
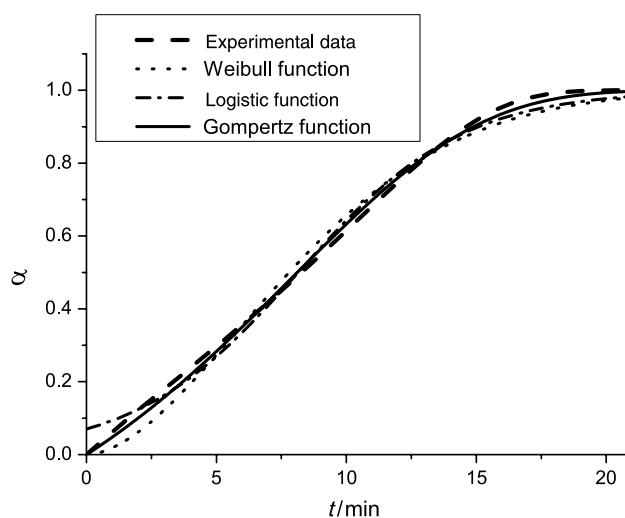

Fig. 10 The fitting of the dehydration conversion curve at 343 K with logistic (Eq. 11), Weibull (Eq. 12), and Gompertz (Eq. 13) function
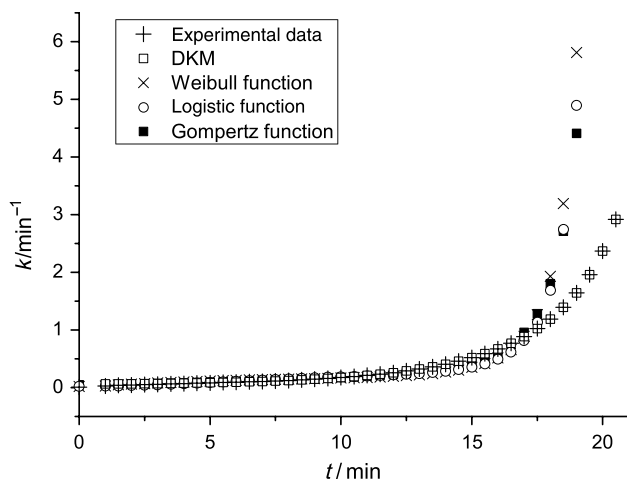
Fig. 11 The fitting of the reaction rate at 343 K with equations for reaction rate obtained from acceleratory DKM (Eq. 10), logistic (Eq. 14), Weibull (Eq. 15), and Gompertz (Eq. 16) function

energy) which confirms that DMK describes the kinetics of PDMAA isothermal dehydration well, and not just fits the conversion curve.

$$k = \frac{b}{1 + e^{-(a + bt)}} \qquad (14)$$

$$k = \frac{\beta}{\eta}\left(\frac{t}{\eta}\right)^{\beta-1} \qquad (15)$$

$$k = abe^{bt} \qquad (16)$$

The results obtained in this paper (i.e. time-dependent activation energy and rate constant) can be also looked at from the point of view of the fluctuating structure of hydrogel. In the case of PDMAA hydrogel dehydration, dehydration leads to continual changes in the structure of absorbed water, as well as in hydrogel itself. Relaxation of structures in absorbed phases and polymer network is slower or comparable to the dehydration process. Due to that, the rate constant of dehydration becomes a time-dependent parameter. Fact that the value of rate constant increases with time indicates that relaxation times of newly formed structures decreases, which is further connected with the formation of dehydration nuclei with different critical radius. According to the dispersive kinetics model, in the case when the rate-limiting step of the process is nucleus formation, the activation energy decreases and is accompanied by an increase in the critical radius [24, 39]. Furthermore, a decrease in activation energy is the consequence of an increase in activation entropy, which is closely related to the mentioned critical radius growth. In the other words, at the beginning of the

dehydration, the smaller critical nuclei (with higher E_a) are formed and as the dehydration process goes on, larger critical nuclei are formed, resulting in dispersion in E_a. On the other hand, the results of Sekine and Ikeda-Fukazawa [30] further confirm this model since the increase in vibrational energies of O–H stretching modes is related to the weakening of hydrogen bonds between the hydrogel and the water which is in accordance with the decreases of the activation energy.

Conclusions

The kinetics of isothermal dehydration of equilibrium swollen poly-*N*,*N*-dimethylacrylamide (PDMAA) hydrogel is complex and thus cannot be well described by commonly used models for the reactions and processes in the solid-state, but neither with the functions which are often used to model processes with nucleation-limited step. Instead, the PDMAA hydrogel dehydration can be only modeled by the acceleratory equation of the dispersive kinetics model (DKM) based on the Maxwell–Boltzmann distribution of activation energies. With an increase in temperature, the model equation parameter *a* decreases, whereas parameter *b* increases exponentially. At all of the investigated temperatures, the value of the rate constant increases with time, while the value of activation energy decreases. Dehydration of PDMAA hydrogel is followed by continual changes in the state of absorbed water within the hydrogel. During the course of dehydration, relaxation processes within the hydrogel become faster. This, according to the DKM, as a consequence has the formation of dehydration nuclei with a bigger critical radius. The presented results are in accordance with literature data on changes state of absorbed water obtained from spectroscopic measurements.

Declarations

References

1. Ahmed EM. Hydrogel: preparation, characterization, and applications: a review. J Adv Res. 2015;6(2):105–21. https://doi.org/10.1016/j.jare.2013.07.006.

2. Majcher MJ, Hoare T. Application of hydrogels. In: Mazumder MAJ, Sherdown H, Al-Ahmed A, editors. Functional biopolimers.

Polymers and polymeric composites: a reference series. Springer; 2019. p. 453–90. https://doi.org/10.1007/978-3-319-95990-0_17.

3. Bashir S, Hina M, Iqbal J, Rajpar AH, Mujataba MA, Alghamda NA, Wageh S, Ramesh K, Ramesh S. Fundamental concepts of hydrogels: synthesis, propertiesm and their application. Polymers. 2020;12(11):2702. https://doi.org/10.3390/polym12112702.

4. Aquino CB, Silva JMR, Oliveira MHR, Coriolano ACF, Delagado RCOB, Fernandes VJ, Araujo AS. Thermogravimetry applied for catalytic degradation of atmospheric residue of petroleum on mesoporous catalyst. J Therm Anal Calorim. 2021;136:2139–44. https://doi.org/10.1007/s10973-018-7830-6.

5. Morandim-Giannetti ADA, Wecchi PDO, Silverio PDA, Carlston R, Bersanetti PA. Attainment and characterization of carboxymethyl chitosan hydrogels by enzymatic cross-linking. J Therm Anal Calorim. 2019;138:3635–43. https://doi.org/10.1007/s10973-019-08571-4.

6. Khalil AM, Rabie ST. Mechanical, thermal and antibacterial performances of acrylonitrile butadiene rubber/polyvinyl chloride loaded with *Moringa oleifera* leaves powder. J Therm Anal Calorim. 2021;143:2973–81. https://doi.org/10.1007/s10973-019-09194-5.

7. Santos FB, Miranda NT, Schiavon MIRB, Fregolente LV, Wolf Maciel MR. Thermal degradation kinetic of poly(acrylamide-co-sodium acrylate) hydrogel applying isoconversional methods. J Therm Anal Calorim. 2020. https://doi.org/10.1007/s10973-020-09899-y.

8. Bae J, Park J, Kim S, Cho H, Kim HJ, Park S, Shin D-S. Tailored hydrogels for biosensor application. J Ind Eng Chem. 2020;89:1–12. https://doi.org/10.1016/j.jiec.2020.05.001.

9. Varaprasad K, Nunez D, Ide W, Jayaramudu T, Sadiku RE. Development of high alginate comprised hydrogel for removal of Pb(II) ions. J Mol Liq. 2020;298: 112087. https://doi.org/10.1016/j.molliq.2019.112087.

10. Ghaffari R, Selimi-Kenari H, Fahimipour F, Rabiee SM, Adeli H, Dashtimoghadam E. Fabrication and characterization of dextran/nanocrystalline β-tricalcium phosphate nanocomposite hydrogel scaffolds. Int J Biol Macromol. 2020;148:434–48. https://doi.org/10.1016/j.ijbiomac.2020.01.112.

11. Baghbadorani NB, Behzad T, Darvanjooghi MHK, Etesami N. Modeling of water adsorption kinetics and biocompatibility study of synthesized cellulose nanofiber-assisted starch-graft-poly(acrylic acid) hydrogel nanocomposites. Cellulose. 2020;27:9927–45. https://doi.org/10.1007/s10570-020-03511-0.

12. Adnađević B, Janković B, Kolar-Anić LJ, Minić D. Normalized weibull distribution function for modelling the kinetics of non-isothermal dehydration of equilibrium swollen poly(acrylic acid) hydrogel. Chem Eng J. 2007;130(1):11–7. https://doi.org/10.1016/j.cej.2006.11.007.

13. Stanković B, Jovanović J, Adnađević B. The kinetics of non-isothermal dehydration of equilibrium swollen Ca-alginate hydrogel. J Therm Anal Calorim. 2020;143:2123–9. https://doi.org/10.1007/s10973-020-10020-6.

14. Adnadjević B, Tasić G, Jovanović J. Kinetic of non-isothermal dehydration of equilibrium swollen poly(acrylic acid-co-methacrylic acid) hydrogel. Thermochim Acta. 2011;512:157–62. https://doi.org/10.1016/j.tca.2010.09.019.

15. Liu L, Wang B, Gao Y, Bai T. Chitosan fibers enhanced gellan gum hydrogels with superior mechanical properties and water-holding capacity. Carbohydr Polym. 2013;97(1):152–8. https://doi.org/10.1016/j.carbpol.2013.04.043.

16. Liu L, Wang B, Bai T, Dong B. Thermal behavior and properties of chitosan fibers enhanced polysaccharide hydrogels. Thermochim Acta. 2014;583:8–14. https://doi.org/10.1016/j.tca.2014.03.008.

17. Ma Y, Bai T, Wang F. The physical and chemical properties of the polyvinylalcohol/polyvinylpyrrolidone/ hydroxyapatite composite

18. Potkonjak B, Jovanović J, Stanković B, Ostojić S, Adnadjević B. Comparative analyses on isothermal kinetics of water evaporation and hydrogel dehydration by a novel nucleation kinetics model. Chem Eng Res Des. 2015;100:323–30. https://doi.org/10.1016/j.cherd.2015.05.032.

19. Jovanović J, Stanković B, Ostojić S, Adnadjević B. Kinetics of isothermal dehydration of equilibrium swollen PAAG hydrogel under the microwave heating conditions. J Therm Anal Calorim. 2017;127:655–62. https://doi.org/10.1007/s10973-016-5440-8.

20. Stankovic B, Jovanovic J, Ostojic S, Adnadjevic B. Kinetic analysis of non-isothermal dehydration of poly(acrylic acid)-g-gelatin hydrogel using distributed activation energy model. J Therm Anal Calorim. 2017;129:541–511. https://doi.org/10.1007/s10973-017-6180-0.

21. Skrdla PJ, Robertson RT. Semiempirical equations for modeling solid-state kinetics based on a Maxwell-Boltzmann distribution of activation energies: applications to a polymorphic transformation under crystallization slurry conditions and to the thermal decomposition of AgMnO4 crystals. J Phys Chem B. 2005;109(21):10611–9. https://doi.org/10.1021/jp045268h.

22. Skrdla PJ, Floyd PD, Dell'Orco PC. Modeling recrystallization kinetics following the dessolution of amorphous drugs. Mol Pharm. 2020;17:219–28. https://doi.org/10.1021/acs.molpharmaceut.9b00940.

23. Wang-Hansen C, Soltani S, Andersson B. Kinetic analysis of O_2- and NO_2-based oxidation of synthetic soot. J Phys Chem C. 2013;117(1):522–31. https://doi.org/10.1021/jp307789r.

24. Skrdla PJ. Modeling sigmoidal transients using dispersive kinetic models to predict nanoparticle size distribution. Cryst Growth Des. 2021;21(3):1843–53. https://doi.org/10.1021/acs.cgd.0c01729.

25. Petri M, Menzel A, Bunk O, Busse G, Techert S. Concentration effects on the dynamics of liquid crystalline self-assembly: time-resolved X-ray scattering studies. J Phys Chem A. 2011;115(11):2176–83. https://doi.org/10.1021/jp1108224.

26. Fu H, Jia C, Chen Q, Cao X, Zhang X. Effect of particle size on the transformation kinetics of flue gas desulfurization gypsum to α-calcium sulfate hemihydrate under hydrothermal conditions. Particuology. 2018;40:98–104. https://doi.org/10.1016/j.partic.2017.10.004.

27. Jin S, Ko K-J, Song Y-G, Lee K, Lee C-H. Fabrication and kinetics study of spherical MgO agglomerates via water-in-oil method for pre-combustion CO_2 capture. Chem Eng J. 2019;359:285–97. https://doi.org/10.1016/j.cej.2018.11.131.

28. Gun'ko VM, Savina UN, Mikhalovsky SV. Properties of water bound in hydrogels. Gels. 2017;3(4):37. https://doi.org/10.3390/gels3040037.

29. Jhon MS, Andrade JD. Water and hydrogels. J Biomed Mater Res. 1973;7(6):509–22. https://doi.org/10.1002/jbm.820070604.

30. Sekine Y, Ikeda-Fukazawa T. Structural changes of water in a hydrogel during dehydration. J Chem Phys. 2009;130: 034501. https://doi.org/10.1063/1.3058616.

31. Naohara R, Narita K, Ikeda-Fukazawa T. Change in hydrogen bonding structures of a hydrogel with dehydration. Chem Phys Lett. 2017;670:84–8. https://doi.org/10.1016/j.cplett.2017.01.006.

32. Algi MP, Okay O. Highly stretchable self-healing poly(*N*, N-dimethylacrylamide) hydrogels. Eur Polym Jour. 2014;59:113–21. https://doi.org/10.1016/j.eurpolymj.2014.07.022.

33. Gudeman LF, Peppas NA. Preparation and characterization of pH-sensitive interpenetrating networks of poly(vinyl alcohol) and poly(acrylic acid). J Appl Polym Sci. 1995;55(6):919–28. https://doi.org/10.1002/app.1995.070550610.

34. Vyazovkin S. Modification of the integral isoconversional method to account for variation in the activation energy. J Comput Chem.

2001;22(2):178–83. https://doi.org/10.1002/1096-987X(20010130)22:2%3c178::AID-JCC5%3e3.0.CO;2-%23.

35. Lazzari S, Pfister D, Diederich V, Kern A, Storti G. Modeling of acrylamide/*N, N′*-methylenebisacrylamide solution copolymerization. Ind Eng Chem Res. 2014;53:9035–48. https://doi.org/10.1021/ie403544d.

36. Baek S, Kim D, Jeon SL, Seo J. Preparation and characterization of pH-responsive poly(*N,N*-dimethylacrylamide-*co*-methacryloyl sulfadimethoxine) hydrogels for application as food freshness indicators. React Funct Polym. 2017;120:57–65. https://doi.org/10.1016/j.reactfunctpolym.2017.09.003.

37. Gao A, Chen S, Yhao S, Zhang G, Cui J, Yan Y. The interaction between *N,N*-dimethylacrylamide and pristine graphene and its role in fabricating a strong nanocomposite hydrogel. J Mater Sci. 2020;55:7652–64. https://doi.org/10.1007/s10853-020-04542-5.

38. Khawam A, Flanagan DR. Solid-state kinetic models: Basics and mathematical fundamentals. J Phys Chem B. 2006;110(35):17315–28. https://doi.org/10.1021/jp062746a.

39. Skrdla PJ. A collision theory-based derivation of semiempirical equations for modeling dispersive kinetics and their application to a mixed-phase crystal decomposition. J Phys Chem A. 2006;10(40):11494–500. https://doi.org/10.1021/jp063534g.

40. Bonilla J, Salazar RP, Mayorga M. Kinetics triplet of Columbian sawmill wastes using thermogravimetric analysis. Heliyon. 2019;5:E02723. https://doi.org/10.1016/j.heliyon.2019.e02723.

41. Muravyev NV, Pivkina AN, Koga N. Critical appraisal of kinetic calculation methods applied to overlapping multistep reactions. Molecules. 2019;24(12):2298. https://doi.org/10.3390/molecules24122298.

42. Sear PR. Quantitative studies of crystal nucleation at constant supersaturation: experimental data and models. Cryst Eng Comm. 2014;16:6506–22. https://doi.org/10.1039/C4CE00344F.